Article

Toward a Molecular Scale Interpretation of Excitation Energy Transfer in Solvated Bichromophoric Systems

Carles Curutchet, and Benedetta Mennucci

J. Am. Chem. Soc., **2005**, 127 (47), 16733-16744• DOI: 10.1021/ja055489g • Publication Date (Web): 08 November 2005

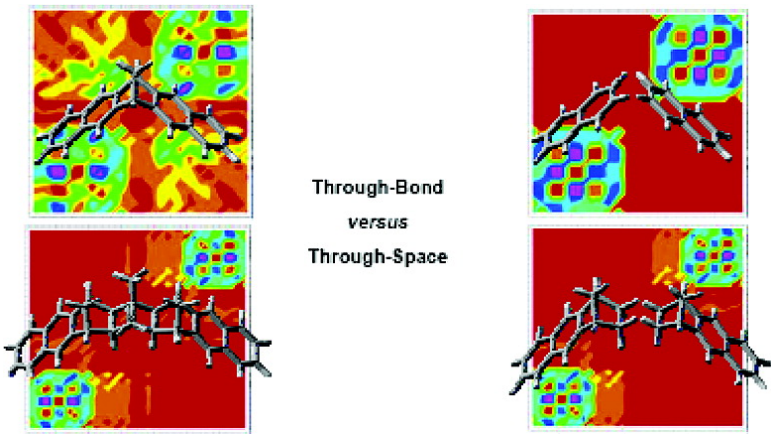

More About This Article

Additional resources and features associated with this article are available within the HTML version:

- Supporting Information
- Links to the 10 articles that cite this article, as of the time of this article download
- Access to high resolution figures
- Links to articles and content related to this article
- Copyright permission to reproduce figures and/or text from this article

View the Full Text HTML

J|A|C|S
ARTICLES
Published on Web 11/08/2005

Toward a Molecular Scale Interpretation of Excitation Energy Transfer in Solvated Bichromophoric Systems

Carles Curutchet and Benedetta Mennucci*

Contribution from the Dipartimento di Chimica e Chimica Industriale, Università di Pisa, via Risorgimento 35, 56126 Pisa, Italy

Received August 22, 2005; E-mail: bene@dcci.unipi.it

Abstract: This paper presents a quantum-mechanical study of the intramolecular excitation energy transfer (EET) coupling in naphthalene-bridge-naphthalene systems in gas phase and in solution. ZINDO and TDDFT response schemes are compared using both an exact and an approximate solution. The approximate solution based on a perturbative approach uses the single chromophore properties to reconstruct the real system coupling thus neglecting possible through-bond effects which conversely are accounted for in the exact solution. The comparison of the results of the two approaches with the experiments allows a detailed analysis of the relative importance of through-bond and through-space effects as well as a more complete understanding of the modifications in the EET coupling with the size of the system, the chromophore−chromophore distance, and solvation.

1. Introduction

The transfer of light from a donor system in an excited electronic state (D^*) to a sensitizer (or acceptor) system (A) with final conversion to chemical energy is performed routinely in nature. Plants use solar antennae to capture incident photons and transmit the excitation energy to reaction centers, where it is used to initiate photosynthesis. This process occurs with an almost perfect efficiency even if it involves a large number of energy-transfer steps characterized by very different time scales and distances. Conversely, there are no synthetic chemical systems that can match this efficiency.[1] It thus becomes of fundamental importance to develop theoretical tools aimed at a better understanding of such a phenomenon to be able to design molecular systems with the required efficiency.

Significative developments in this direction started more than 50 years ago, when Förster introduced a method for calculating the excitation energy transfer (EET) rate between molecules from the overlap of the donor molecule's fluorescence spectrum and the acceptor molecule's absorption spectrum.[2] This theory has had an enormous impact on biology, chemistry, and physics. However, ultrafast spectroscopy and (quantum chemical) calculations have shown that many energy transfers cannot be correctly characterized by conventional Förster theory, which is based on the representation of the interchromophore coupling as a Coulombic interaction between donor and acceptor transition dipoles.[3,4] Many different approaches have been proposed to complement or substitute such a theory, for example, by introducing Dexter exchange,[5] super exchange,[6] and through-bond (TB) interaction[7,8] depending on the nature of the $D-A$ systems, their relative distance, and the possible presence of real chemical bonds between them. The EET process in fact can also occur intramolecularly, that is, between two bridged parts of a molecule. Intramolecular EET processes are of very large importance from both a modelistic and an applied point of view.[9,10] On one hand, with an intra-EET process, control of the spatial relationship between donor and acceptor groups may exist without the randomness characteristic of intermolecular interactions. On the other hand, intra-EET can be observed in rigid or viscous media where encounters between separated molecules leading to short-range EET are not possible. In addition, a rigid bridge will make the energy transfer much more efficient and tunable thus permitting us to build intramolecular logic gates or molecular machines.

Bichromophoric molecules are ideal for investigating intra-EET processes. By using the powerful tools of synthetic organic and polymer chemistry, molecular systems can be engineered for a specific intra-EET study. For the particular purpose of elucidating the mechanism of short-range intra-EET in bichromophoric molecules, the interchromophore bridge should act as an inert spacer, minimizing any coupling between the ground electronic states of the two chromophores, allowing, however, for weak coupling between D^* and A to promote short-range intra-EET. Moreover, the bridge should be rigid enough to

(1) Fleming, G. R.; Scholes, G. D. *Nature* **2004**, *431*, 256.
(2) Forster, T. *Annalen der Physik* **1948**, *2*, 55.
(3) Scholes, G. D. *Annu. Rev. Phys. Chem.* **2003**, *54*, 57.
(4) (a) *Resonance Energy Transfer*; Andrews, D. L., Demidov, A. A., Eds.; Wiley: New York, 1999. (b) May, V.; Kühn, O. *Charge and Energy Transfer Dynamics in Molecular Systems*; Wiley-VCH: Berlin, 2000.
(5) Dexter, D. L. J. *Chem. Phys.* **1953**, *21*, 836.
(6) (a) Monberg, E. M.; Kopelman, R. *Chem. Phys. Lett.* **1978**, *58*, 492. (b) Klafter, J.; Jortner, J. *Chem. Phys. Lett.* **1978**, *60*, 5.
(7) (a) McConnell, H. M. *J. Chem. Phys.* **1961**, *35*, 508. (b) Hoffmann, R.; Imamura, A.; Hehre, W. J. *J. Am. Chem. Soc.* **1967**, *90*, 1499. (c) Hoffmann, R. *Acc. Chem. Res.* **1971**, *4*, 19.
(8) (a) Paddon-Row, M. N. *Acc. Chem. Res.* **1982**, *15*, 245. (b) Paddon-Row, M. N.; Wong, S. S.; Jordan, K. D. *J. Am. Chem. Soc.* **1990**, *112*, 1710. (c) Jordan, K. D.; Paddon-Row, M. N. *Chem. Rev.* **1992**, *92*, 395. (d) Shephard, M. J.; Paddon-Row, M. N.; Jordan, K. D. *J. Am. Chem. Soc.* **1994**, *116*, 5328.
(9) Speiser, S. *Chem. Rev.* **1996**, *96*, 1953.
(10) Speiser, S. *J. Lumin.* **2003**, *102*, 267.

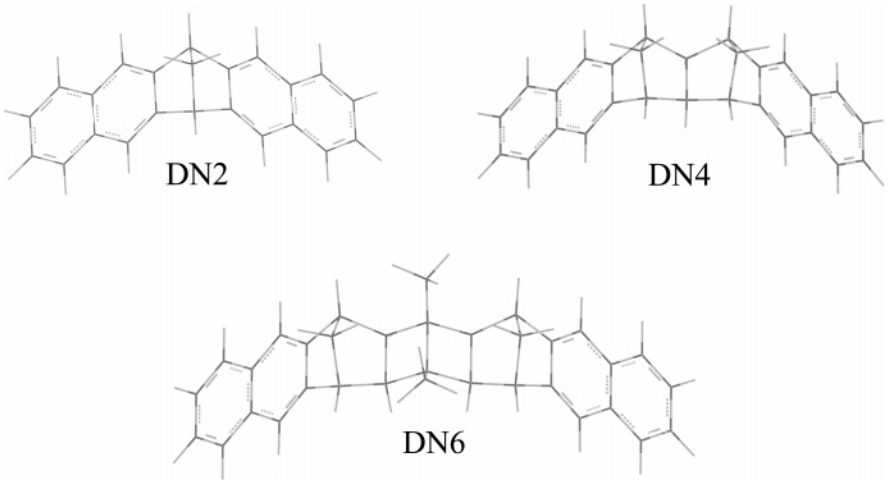

Figure 1. Structures of naphthalene-bridge-naphthalene systems DN2, DN4, and DN6.

provide a controlled geometrical relationship between the chromophores and to allow for only a limited number of molecular conformations. Naphthalene, anthracene, and their derivatives comprise a class of particularly well studied aromatic molecules that may undergo EET while in their excited state. In particular, the family of naphthalene-bridge-naphthalene systems DN2, DN4, and DN6 have been largely studied. These molecules may be regarded as naphthalene dimers where pairs of naphthalene chromophores are held at fixed distances and orientations by a rigid polynorbornyl-type bridge of variable length, two, four, or six bonds, respectively (see Figure 1).

The UV spectra and radiative decay rates of these dimers have been measured[11−13] and interpreted by using different QM approaches.[11,14,15] Traditionally, for the intra-EET process a distinction is introduced between through-space (TS) contributions and through-bond (TB) or intrabond contributions induced by the bridge. TS terms are originated either by a Coulombic interaction between the transition densities of each chromophore (approximated by a dipole−dipole term in Förster theory) or by an exchange (Dexter) interaction originated by a direct through-space orbital overlap between transition densities. On the other hand, TB contributions include charge-transfer effects mediated by the bridge that lead to electronic delocalization of the excitation between the chromophores.

Following this modelistic framework, Ghiggino and collaborators[11] found that for the two-bond bridged compound a description of the exciton interaction requires consideration of "direct through-space orbital overlap" (involving charge transfer) between naphthalenes, whereas these overlaps are negligible in the four-bond and the six-bond bridged compounds. For these latter, a significant contribution is instead represented by a through-bond interaction (involving the σ- and σ*-orbitals of the bridge) which leads to the efficient delocalization of the excitation.

More recently, Mukamel and co-workers[15] have further analyzed the same systems by applying their CEO/INDO/S approach.[16] They found that, for DN6, the dimer states are combinations of the monomer excited state wave functions and the interaction between monomers is purely electrostatic and relatively weak (and thus in this case the exciton model perfectly works); for DN4, a weak exchange (Dexter) interaction starts to show up (and thus the exciton model is therefore only marginally applicable); and for DN2, a large electronic delocalization between chromophores (i.e., charge separation processes where the electron and hole reside on different monomers become allowed) is active, and this leads to a complete failure of the exciton model.

These analyses seem thus to show a quite different mechanism acting along the DNX series of compounds; we have to note however that two important aspects have been neglected or not accurately analyzed in these previous studies, namely the effects of the solvent and those of the QM level of description.

As regards the effects of the solvent on EET processes, Förster originally recognized their importance. His idea was that the electronic coupling, approximated as the Coulomb interaction between donor and acceptor, is screened by the presence of the dielectric. Such a screening, however, is just an approximation of a part of the global effect induced by a polarizable environment on the EET process. The presence of a solvent in fact not only screens the Coulomb interactions as formulated by Förster, but it also affects all the electronic properties of the interacting donor and acceptor (for a clear analysis of this aspect, see for example ref 18).

Concerning the effects of the QM level of calculation, we have to note that, due to the large dimensions of the molecular systems of greater interest for EET, QM studies have started to appear only much later than the first theoretical formulations. An important impulse has been represented by response theories[17] in which we do not need to explicitly determine the electronic excited states involved in the transfer but just the response of the ground state to an external perturbation. The application of these theories to EET (which is based on the implicit assumption that the energy transfer occurs more rapidly than any molecular motion) has made the QM description

(11) Scholes, G. D.; Ghiggino, K. P.; Oliver, A. M.; Paddon-Row, M. N. *J. Am. Chem. Soc.* **1993**, *115*, 4345.
(12) Clayton, A. H. A.; Ghiggino, K. P.; Lawson, J. M.; Paddon-Row, M. N. *J. Photochem. Photobiol., A* **1994**, *80*, 323.
(13) Scholes, G. D.; Turner, G. O.; Ghiggino, K. P.; Paddon-Row, M. N.; Piet, J. J.; Schuddeboom, W.; Warman, J. M. *Chem. Phys. Lett.* **1998**, *292*, 601.
(14) Clayton, A. H. A.; Scholes, G. D.; Ghiggino, K. P.; Paddon-Row, M. N. *J. Phys. Chem.* **1996**, *100*, 10912.
(15) Tretiak, S.; Zhang, W. M.; Chernyak, V.; Mukamel, S. *Proc. Natl. Acad. Sci. U.S.A.* **1999**, *96*, 13003.
(16) Tretiak, S.; Mukamel, S. *Chem. Rev.* **2002**, *102*, 3171.
(17) (a) McWeeny, R. *Methods of Molecular Quantum Mechanics*, 2nd ed.; Academic: London, 1992. (b) Olsen, J.; Jorgensen, P. In *Modern Electronic Structure Theory, Part II*; Yarkony, D. R., Ed.; World Scientific: Singapore, 1995.
(18) Knox, R. S.; van Amerongen, H. *J. Phys. Chem. B* **2002**, *106*, 5289. (b) Knox, R. S. *Photochem. Photobiol.* **2003**, *77*, 492.

feasible also for quite large systems. In particular, the semiempirical versions of this approach, such as the previously cited CEO/INDO/S or the ZINDO approach,[21] have been largely used.[19,20] Alternatively,[22−25] more accurate QM descriptions such as Hartree−Fock (HF) or Density Functional Theory (DFT) have been used in their extensions to response theories, namely the Tamm−Damcoff approximation (TDA or CIS)[26] and the time-dependent DFT (TDDFT).[27]

Following these most recent developments, here we present a QM study of the electronic coupling in DNX systems by comparing the semiempirical ZINDO with the more complete TDDFT and accounting for solvent effects in all the steps of the QM calculations.[28,29]

The model used to include solvent effects is the integral equation formalism (or IEF)[30] version of the polarizable continuum model (PCM).[31] In the IEFPCM model, the effects of the medium on a QM molecular system (from now on indicated as the "solute") is introduced by describing the solvent as a structureless continuum, characterized by its macroscopic dielectric permittivity, and defining a proper separation between the two parts of the system. The resulting boundary (the cavity surface) is then used to represent the polarization effects induced by the solute expressed as a *reaction field* originated by *apparent surface charges* displaced on the cavity surface.[32]

To better analyze the real nature of the EET in DNX systems and to quantify the relative importance of the various interactions determining such a process (Coulomb, exchange, overlap, through-bond, and solvent interactions), we exploit both an exact and an "approximated" solution of the TDDFT (or ZINDO) equation for both isolated and solvated DNX systems. The approximated model, which perturbatively solves the TDDFT (or ZINDO) equation, resembles the conventional exciton theories in which the interactions between *D* and *A* are considered as a slight perturbation and therefore the excited states of the total system are expressed on the basis of the electronic wave functions of the individual unperturbed systems. Here, however, both the properties of the unperturbed systems and their coupling are evaluated in the presence of the solvent.[33]

The paper is organized as follows. In section 2 we briefly describe the theoretical methods employed and the related computational details. In section 3, we verify the reliability and the accuracy of both the QM level and the solvation model by comparing naphthalene excitation energies with experimental absorption spectra. In section 4 we present the results obtained for the EET coupling of the DNX systems using the perturbative TDDFT (and ZINDO) schemes, and we discuss them in terms of through-space and through-bond contributions in section 5. In section 6 we recompute the coupling using the "exact" solution (also indicated as supermolecule approach), and in section 7 we present an analysis of all the results using transition density contour plots. Finally, in section 8 we report a short summary.

2. Methods

2.1. Quantum Mechanical Theory. The presentation of the perturbative TDDFT (or ZINDO) approach for the description of EET within the IEFPCM approach has been already published;[33] here however we repeat some of the most important aspects to allow the reader a more complete comprehension of the results we shall report in the following sections.

The starting point is to consider two solvated chromophores, *A* and *D*, with a common resonance frequency, ω_0, when not interacting. When their interaction is turned on, their respective transitions are no longer degenerate. By contrast, two distinct transition frequencies ω_+ and ω_- appear. The splitting between these defines the energy transfer coupling,

$$J = \frac{[\omega_+ - \omega_-]}{2} \tag{1}$$

and it can be evaluated by computing the excitation energies of the $D \oplus A$ system through a proper TDDFT (or ZINDO) scheme. Namely by solving[27]

$$\begin{pmatrix} \mathbf{A} & \mathbf{B} \\ \mathbf{B}^* & \mathbf{A}^* \end{pmatrix} \begin{pmatrix} \mathbf{X}_n \\ \mathbf{Y}_n \end{pmatrix} = \omega_n \begin{pmatrix} 1 & 0 \\ 0 & -1 \end{pmatrix} \begin{pmatrix} \mathbf{X}_n \\ \mathbf{Y}_n \end{pmatrix} \tag{2}$$

where the matrices **A** and **B** form the Hessian of the electronic energy for the whole $D \oplus A$ system and the transition vectors ($\mathbf{X}_n$ $\mathbf{Y}_n$) correspond to collective eigenmodes of the density matrix with eigenfrequencies ω_n. The Coulombic and exchange-correlation (XC) kernels produce both diagonal and off-diagonal contributions to **A** and **B**, correcting the transitions between occupied and unoccupied levels of the ground-state potential into the true transitions of the system. Inclusion of IEFPCM solvent effects into the **A** and **B** matrices is possible by considering the apparent surface charges induced by the density matrix associated with the transition vectors ($\mathbf{X}_n\mathbf{Y}_n$).[28]

By using the usual convention in labeling MOs (i.e., (*i*, *j*, ...) for occupied; (*a*, *b*, *c*, ...) for virtual), the matrices **A** and **B** thus become

$$A_{ai,bj} = \delta_{ab}\delta_{ij}(\epsilon_a - \epsilon_i) + K_{ai,bj} + \mathscr{B}^{IEF}_{ai,bj}$$
$$B_{ai,bj} = +K_{ai,jb} + \mathscr{B}^{IEF}_{ai,bj} \tag{3}$$

(19) Tretiak, S.; Chernyak, V.; Mukamel, S. *J. Phys. Chem. B* **1998**, *102*, 3310. Tretiak, S.; Middleton, C.; Chernyak, V.; Mukamel, S. *J. Phys. Chem. B* **2000**, *104*, 9540.

(20) (a) Ottonelli, M.; Musso, G.; Comoretto, D.; Dellepiane, G. *J. Phys. Chem. B* **2005**, *109*, 5485. (b) Ortiz, W.; Roitberg, A. E.; Krause, J. L. *J. Phys. Chem. B* **2004**, *108*, 8218. (c) Jordanides, X. J.; Scholes, G. D.; Shapley, W. A.; Reimers, J. R.; Fleming, G. R. *J. Phys. Chem. B* **2004**, *108*, 1753. (d) Ng, M.-F.; Zhao, Y.; Chen, G.-H. *J. Phys. Chem. B* **2003**, *107*, 9589.

(21) (a) Bacon, A. D.; Zerner, M. C. *Theor. Chim. Acta* **1979**, *53*, 21. (b) Correa de Mello, P.; Hehenberger, M.; Zerner, M. C. *Int. J. Quantum Chem.* **1982**, *21*, 251. (c) Zerner, M. C. *J. Chem. Phys.* **1975**, *62* (7), 2788. (d) Zerner, M. C. *Reviews in Computational Chemistry*; Lipkowitz, K. B., Boyd, D. B., Eds.; VCH Publishing: New York, 1991; Vol. 2, p 313.

(22) (a) Scholes, G. D.; Gould, I. R.; Cogdell, R. J.; Fleming, G. R. *J. Phys. Chem. B* **1999**, *103*, 2543. (b) Krueger, B. P.; Scholes, G. D.; Fleming, G. R. *J. Phys. Chem. B* **1998**, *102*, 5378.

(23) (a) Hsu, C.-P.; Walla, P. J.; Head-Gordon, M.; Fleming, G. R. *J. Phys. Chem. B* **2001**, *105*, 11016. (b) Dreuw, A.; Fleming, G. R.; Head-Gordon, M. *J. Phys. Chem. B* **2003**, *107*, 6500. (c) Dreuw, A.; Fleming, G. R.; Head-Gordon, M. *Phys. Chem. Chem. Phys.* **2003**, *5*, 3247. (d) Dreuw, A.; Head-Gordon, M. *J. Am. Chem. Soc.* **2004**, *126*, 4007.

(24) (a) Yamaguchi, Y.; Yokomichi, Y.; Yokoyama, S.; Mashiko, S. *Int. J. Quantum Chem.* **2001**, *84*, 338. (b) Yamaguchi, Y.; Yokoyama, S.; Mashiko, S. *J. Chem. Phys.* **2002**, *116*, 6541

(25) Polivka, T.; Zigmantas, D.; Herek, J. L.; He, Z.; Pascher, T.; Pulleritis, T.; Cogdell, R. J.; Frank, H. A.; Sundstrom, V. *J. Phys. Chem. B* **2002**, *106*, 11016

(26) (a) Hirata, S.; Head-Gordon, M. *Chem. Phys. Lett.* **1999**, *314*, 291. (b) Foresman, J. B.; Head-Gordon, M.; Pople, J. A.; Frisch, M. J. *J. Phys. Chem.* **1992**, *96*, 135.

(27) (a) Casida, M. E. In *Recent Advances in Density Functional Methods*; Chong, D. P., Ed.; World Scientific: Singapore, 1995; Part I. (b) Gross, E. U. K.; Dobson, J. F.; Petersilka, M. In *Density Functional Theory II*; Nalewajski, R. F., Ed.; Springer: Heidelberg, 1996.

(28) (a) Cammi, R.; Mennucci, B. *J. Chem. Phys.* **1999**, *110*, 9877. (b) Cammi, R.; Mennucci, B.; Tomasi, J. *J. Phys. Chem. A* **2000**, *104*, 5631.

(29) Caricato, M.; Mennucci, B.; Tomasi, J. *J. Phys. Chem. A* **2004**, *108*, 6248.

(30) (a) Cancès, E.; Mennucci, B. *J. Math. Chem.* **1998**, *23*, 309. (b) Cancès, E.; Mennucci, B.; Tomasi, J. *J. Chem. Phys.* **1997**, *107*, 3031. (c) Mennucci, B.; Cancès, E.; Tomasi, J. *J. Phys. Chem. B* **1997**, *101*, 10506.

(31) (a) Miertus, S.; Scrocco, E.; Tomasi, J. *Chem. Phys.* **1981**, *55*, 117. (b) Cammi, R.; Tomasi, J. *J. Comput. Chem.* **1995**, *16*, 1449.

(32) Tomasi, J.; Mennucci, B.; Cammi, R. *Chem. Rev.* **2005**, *105*, 2999.

(33) Iozzi, M. F.; Mennucci, B.; Tomasi, J.; Cammi, R. *J. Chem. Phys.* **2004**, *120*, 7029.

where ϵ_r are the orbital energies, $K_{ai,bj}$ and $\mathcal{B}^{IEF}_{ai,bj}$ are the coupling matrix and the solvent matrix, respectively,

$$K_{ai,bj} = \int d\mathbf{r} \int d\mathbf{r}' \phi_i(\mathbf{r}') \phi_a^*(\mathbf{r}') \left(\frac{1}{|\mathbf{r}' - \mathbf{r}|} + g_{xc}(\mathbf{r}',\mathbf{r})\right) \phi_j(\mathbf{r}) \phi_b^*(\mathbf{r}) \quad (4)$$

$$\mathcal{B}^{IEF}_{ai,bj} = \sum_k \left(\int d\mathbf{r}\, \phi_i(\mathbf{r}') \phi_a^*(\mathbf{r}') \frac{1}{|\mathbf{r}' - \mathbf{s}_k|} \right) q(\mathbf{s}_k; \epsilon_\omega, \phi_j\phi_b^*) \quad (5)$$

and g_{xc} is the exchange-correlation kernel. In eq 5 the k index runs on the total number of apparent surface charges $q(\mathbf{s}_k)$, and ϵ_ω is the solvent frequency-dependent dielectric permittivity. We note that for ZINDO *xc* terms in eq 4 become zero and the whole matrix **B** is neglected while the form of the solvent terms is not changed.[29]

The alternative strategy used in the approximate model does not solve the system (2) exactly, but instead it introduces a perturbative approach[34] which considers the *D*/*A* interaction as a perturbation and defines the zero-order resulting eigenvectors, $(\mathbf{X}_+\mathbf{Y}_+)$ and $(\mathbf{X}_-\mathbf{Y}_-)$, as linear combinations of the unperturbed Kohn−Sham orbitals of the two separated *D* and *A* systems.[34] Within this approximation, the splitting and the corresponding coupling can be obtained (at first order) by knowing the transition densities of the systems *D* and *A* in the absence of their interaction.

To include solvent effects into this scheme, we define an effective coupling matrix, which couples transitions of *D* with those of *A* in the presence of a third body represented by the IEF dielectric medium.[33] As a result, the first-order approximation of the coupling, $J^{(1)}$, becomes a sum of two terms, one which is always present (i.e., also in isolated systems) and another which has an explicit dependence on the medium, namely:

$$J^{(1)} = J^0 + J^{IEF} \quad (6)$$

$$J^0 = \int d\mathbf{r} \int d\mathbf{r}'\, \rho_D^{T*}(\mathbf{r}') \left(\frac{1}{|\mathbf{r}' - \mathbf{r}|} + g_{xc}(\mathbf{r}',\mathbf{r})\right) \rho_A^T(\mathbf{r}) - \omega_0 \int d\mathbf{r}\, \rho_D^{T*}(\mathbf{r})\, \rho_A^T(\mathbf{r}) \quad (7)$$

$$J^{IEF} = \sum_k \left(\int d\mathbf{r}\, \rho_D^{T*}(\mathbf{r}) \frac{1}{|\mathbf{r} - \mathbf{s}_k|} \right) q(s_k; \epsilon_\omega, \rho_A^T) \quad (8)$$

where ρ_D^T and ρ_A^T indicate transition densities of the solvated systems *D* and *A*, respectively. In particular, J^0 describes a solute−solute Coulomb and exchange-correlation interaction corrected by an overlap contribution. We note that when a ZINDO Hamiltonian is used the exchange-correlation and the overlap terms become zero.

The effects of the solvent on J^0 are implicitly included in the values of the transition properties of the chromophores before the interaction between the two is switched on. These properties can in fact be significantly modified by the "reaction field" produced by the polarized solvent. In addition, the solvent explicitly enters into the definition of the coupling through the term J^{IEF} of eq 8 which describes the solvent screened chromophore−chromophore interaction. More details on these double effects of the solvent (one implicit on transition properties of each chromophore, and one explicit on the chromophore−chromophore interactions) can be found in the reference paper on the presentation of the IEFPCM model for EET,[33] as well as in the papers by Knox and co-workers on the refractive index dependence of the EET rate.[18]

The numerical advantage of the perturbative approach with respect to the standard one in which we have to solve the TD scheme for the supermolecule $(D + A)$ is that only the properties of the single solvated chromophores (*D* and *A*) are required to get the coupling. The computational strategy can be thus split into two subsequent separate steps. First ρ_X^T are evaluated through a TDDFT scheme applied to each single chromophore (in the symmetric case of $A \equiv D$, a single TDDFT problem has to be solved). Once ρ_X^T are known, the coupling is obtained as a sum of integrals defined in the $D \oplus A$ functional space. The heavy calculation is thus limited to the first step (on the single chromophore), since the second step consists of only the calculations of integrals which can be performed with standard numerical integration techniques.

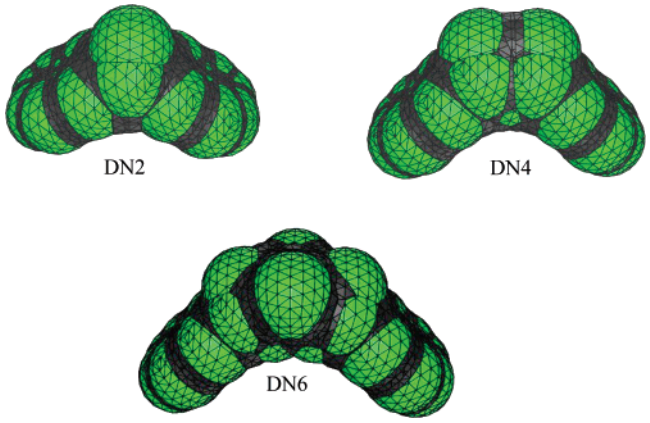

Figure 2. IEFPCM cavities used for the three DNX systems.

2.2. Computational Details. Geometry optimizations of naphthalene and naphthalene-bridge-naphthalene systems (DN2, DN4, and DN6) were performed both at the density functional theory (DFT) and at the AM1 semiempirical levels in gas phase. For DFT optimizations, the 6-31G(d,p) basis set was used along with the common B3LYP hybrid functional which mixes the Lee, Yang, and Parr functional for the correlation part and Becke's three-parameter functional for the exchange.[35] Due to the rigidity of the systems and the low polarity of the solvent here considered (namely hexane), minor effects are expected to arise from changes in solvated structures, which justifies the use of gas-phase geometries.

EET couplings for the bridged-naphthalene dimers as well as the naphthalene absorption spectrum were then computed both in vacuo and in *n*-hexane solution at the TDDFT:B3LYP/6-31+G(d,p) level of theory and using the INDO/S Hamiltonian in the CIS framework, i.e., the ZINDO[21] approach (using DFT or AM1 optimized geometries, respectively). For ZINDO a complete active space has been used. "Supermolecule" calculations were carried out using the entire systems, while for the perturbative approach different models for the *D*/*A* pair were tested. These models were obtained from the structures of the real systems by simply eliminating atoms but keeping all the rest frozen (see section 4).

For all the solvated systems the IEFPCM solvation model was used and the molecular cavities were obtained in terms of interlocking spheres centered on selected nuclei. The chosen radii were 2.0 Å for the methylene group, 1.9 Å for the CH group, and 1.7 Å for carbon atoms.[36] All the radii were multiplied by a factor equal to 1.2 in order to take into account the fact that atomic bond or lone pair centers of the solvent molecules are normally located a bit further from the solute atoms than a van der Waals radius.[37] The resulting IEFPCM cavities for the three DNX systems are reported in Figure 2.

Finally, a macroscopic relative permittivity (both static and dynamic) of 1.88 was used for *n*-hexane in IEFPCM calculations.

All QM calculations both in vacuo and in solution were performed using a local version of the Gaussian 03 code[38] properly modified to perform the perturbative approach and to extract the quantities required to plot the transition densities.

(34) Hsu, C.-P.; Fleming, G. R.; Head-Gordon, M.; Head-Gordon, T. *J. Chem. Phys.* **2001**, *114*, 3065.
(35) (a) Becke, A. D. *J. Chem. Phys.* **1993**, *98*, 5648. (b) Lee, C.; Yang, W.; Parr, R. G. *Phys. Rev. B* **1988**, *37*, 785.
(36) Bondi, A. *J. Phys. Chem.* **1964**, *68*, 441.
(37) Tomasi, J.; Persico, M. *Chem. Rev.* **1994**, *94*, 2027.
(38) Frisch, M. J. et al. *Gaussian 03*, revision C.02; Gaussian, Inc.: Pittsburgh, PA, 2003.

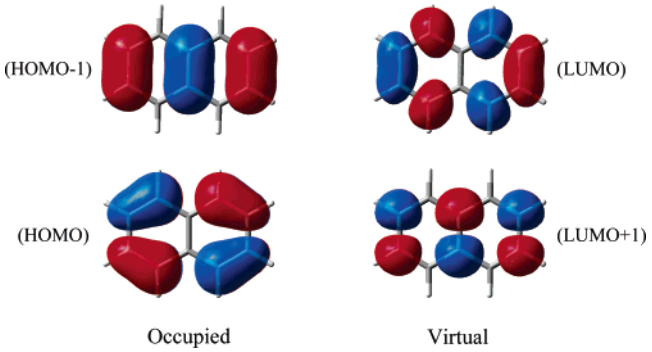

Figure 3. Occupied (HOMO and HOMO−1) and virtual (LUMO and LUMO+1) orbitals involved in the three lowest naphthalene singlet transitions (at the ZINDO level).

3. A Preliminary Test on Naphthalene Absorption Spectrum

Before passing to analyze EET processes we have made a preliminary test on both the QM level of calculation and the solvation model. We have thus computed excitation energies for naphthalene in gas phase and in hexane solution by using ZINDO and TDDFT approaches.

Experimentally, three electronic transitions (all of $\pi \rightarrow \pi^*$ character) are seen in the near-UV region for naphthalene both in the vapor phase[39] and in an apolar solvent.[40] Assuming D_{2h} symmetry for naphthalene, which is placed into the *xy* plane with the long molecular axis along the *x*-direction, the first (very weak) transition is to an excited singlet state of B_{3u} symmetry with energy at about 3.95 eV and presenting a very small solvatochromic shift. The next two transitions (with moderate and high intensities, respectively) are to excited singlet states of B_{2u} and B_{3u} symmetry. Both present a not negligible solvent-induced red-shift.

All the three transitions present two main contributions each; the involved occupied (HOMO, and HOMO−1) and virtual (LUMO and LUMO+1) orbitals (at ZINDO level) are reported in Figure 3.

The intense B_{3u} transition, characterized by HOMO → LUMO+1 and HOMO−1 → LUMO contributions, presents transition dipole moments along the naphthalene long axis (here *x*), while, in the B_{2u}, characterized by the complementary HOMO−1 → LUMO+1 and HOMO → LUMO contributions, the transition dipole moment is along the short axis (here *y*). The very weak B_{3u}, characterized by an equivalent but complementary combination of orbitals with respect to the intense B_{3u}, presents a negligible transition dipole.

The calculated and experimental excitation energies are reported in Table 1 together with the corresponding oscillator strengths.

As can be seen, the TDDFT approach accurately describes the two more intense transitions, while ZINDO gives a better value for the other weak transition; for all the transitions, both approaches give correct solvent shifts. In particular an almost null shift is found for the lower B_{3u}, whereas a significant red-shift (0.21 eV for TDDFT and 0.26 eV for ZINDO) is found for the higher and intense B_{3u} transition: both results are in very good agreement with what was experimentally observed.

(39) George, G. A.; Morris, G. C. *J. Mol. Spectrosc.* **1968**, *26*, 67.
(40) Klevens, H. B.; Platt, J. R. *J. Chem. Phys.* **1949**, *17*, 470.

Table 1. Calculated (ZINDO and TDDFT) Excitation Energies (in eV) for the First Singlet States of Naphthalene in Gas and in Solution

	ZINDO//AM1	TDDFT//DFT	expt
	in gas		ref 39
$1B_{2u}$	4.22 (0.147)	4.37 (0.081)	4.45 (0.1)
$1B_{3u}$	3.98 (0.004)	4.45 (0.000)	3.97 (0.002)
$2B_{3u}$	5.29 (1.630)	5.85 (1.260)	5.89 (1.3)
	in hexane		ref 40[a]
$1B_{2u}$	4.17 (0.194)	4.34 (0.084)	4.34 (0.2)
$1B_{3u}$	3.98 (0.007)	4.45 (0.000)	3.94 (0.002)
$2B_{3u}$	5.03 (1.657)	5.64 (1.462)	5.62 (1.2)

[a] Experimental values are obtained in *n*-heptane.

The results reported in Table 1, and in particular those found for the $2B_{3u}$ transition (i.e., that giving rise to the observed splitting), clearly show the reliability and the accuracy of the TDDFT approach (and of the IEFPCM-TDDFT combination) in the study of excitation energies of the naphthalene moiety,[41] and they thus make us confident in the applicability of the perturbative TDDFT model to the DNX series. A different situation is found for ZINDO (and IEFPCM-ZINDO), as in this case the accuracy is significantly worse (a 0.6 eV error is found both in gas and in hexane); in the following we shall show how these limitations are reflected in the EET couplings of DNX systems.

4. The Perturbative Approximation

We now turn to the polynorbornyl-bridged naphthalene dimer series (DN2, DN4, and DN6) with varying interchromophore distances (Figure 1). The experimental UV spectra of DNX systems in hexane[11−13] clearly show the dimeric splitting resulting from the major naphthalene absorption band $A_g \rightarrow 2B_{3u}$. With increasing the bridge length (from DN2 to DN6), the two primary peaks get closer, indicating that the coupling becomes smaller, as expected. The experimentally observed splittings are 0.758, 0.442, and 0.198 eV for DN2, DN4, and DN6, respectively. Other peaks in these spectra (e.g., the low-frequency features) could not be easily identified and linked to monomer transitions.

To try to reproduce the observed splittings we have first applied the perturbative method described in section 2.2. Both ZINDO and TDDFT:B3LYP/6-31+G(d,p) levels have been used with and without the inclusion of the IEFPCM solvation model.

Different models have been tested to represent the *D*/*A* pair starting from the simplest one, two naphthalenes (here indicated as "Naphtha"), and then enlarging it by including "pieces" of the polynorbornyl-type bridge; obviously such enlarged models are possible only for the longer DN4 ("Bridge1") and DN6 ("Bridge1" and "Bridge2") systems. These models, which are reported in Figures 4−6, have been obtained from the structures of the corresponding real DNX systems by eliminating bridge atoms but keeping all the rest frozen. The hydrogen atoms introduced to saturate valences of the carbon atoms bonded to the cut atoms have standard bond lengths. In the same figures we also report the inter-naphthalene distances in the three DNX systems (such distances differ by less than 0.01 Å when obtained at the AM1 or B3LYP level of geometry optimization). It is

(41) (a) Heinze, H. H.; Gorling, A.; Rosch, N. *J. Chem. Phys.* **2000**, *113*, 2088. (b) Adamo, C.; Scuseria, G. E.; Barone, V. *J. Chem. Phys.* **1999**, *111*, 2889.

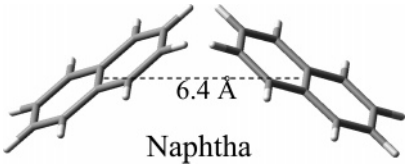

Figure 4. Molecular model used to represent the *D*/*A* pair in the perturbative calculation of DN2.

worth recalling that the molecular cavities used in IEFPCM perturbative calculations were those of the corresponding real DNX systems (see Figure 2) and not the cavities of the single monomers of the various model systems; in fact, the use of monomeric cavities would lead to artificial solvent effects due to the part of such cavities which would be exposed to the solvent while it is occupied by the rest of the molecule in the corresponding real systems.

In Table 2 we report the perturbative coupling ($J^{(1)}$) values obtained by calculating the transition density of the *Donor* of each model system (here in fact $\rho_A^T = \rho_D^T$) using ZINDO//AM1 and TDDFT//DFT descriptions and combining it according to eq 6. Note that with using a ZINDO Hamiltonian only the Coulomb (and the IEFPCM) terms survive.

The results reported in Table 2 first show the importance of the solvent effects, which always lead to a smaller coupling (and thus to a smaller splitting). This behavior is not unexpected as the solvent used here, the apolar *n*-hexane, cannot induce a strong polarization of the interacting systems but still it can screen their interaction and thus lead to a decrease of the coupling with respect to the gas-phase systems.

Passing to a comparison of the different models adopted for DN4 and DN6, we find that the enlargement of the interacting moieties leads to a better agreement with experiments: this is due to the changes in the electronic properties of naphthalene because of the (poly)norbornane group, which breaks the symmetry of naphthalene and causes significant modifications in the oscillator strengths. The results reported in Table 2 show that these changes, already put in evidence by Mukamel and co-workers,[15] significantly affect the coupling especially at the TDDFT level; for example for the solvated DN6 we double the coupling passing from the simplest "Naphtha" model to the most complete "Bridge2". This result is relevant as it shows that the effects of the bridge are composed by different contributions not limited to real "through bond" charge transfers between the two moieties but also including modifications of the electronic character of the *D* (and *A*) due to the presence of bonded groups. This combination of distinct but linked terms will be further discussed in section 5.

Table 2. Perturbative ZINDO and TDDFT $J^{(1)}$ (in eV) Obtained Using Different Model Systems (Naphtha, Bridge1, and Bridge2; See Figures 4−6)[a]

	ZINDO			TDDFT			
	Naphtha	Bridge1	Bridge2	Naphtha	Bridge1	Bridge2	expt[b]
	in gas			in gas			
DN2	0.185			0.213			NA
DN4	0.083	0.108		0.095	0.123		NA
DN6	0.042	0.053	0.066	0.043	0.061	0.078	NA
	in hexane			in hexane			
DN2	0.155			0.201			0.379
DN4	0.055	0.075		0.075	0.109		0.221
DN6	0.024	0.031	0.041	0.030	0.047	0.064	0.099

[a] Both gas-phase and solvated results are reported. In the latter case experimental data are also shown. [b] Reference 11.

Going into a more detailed analysis we observe that the general trends are qualitatively recovered by the perturbative

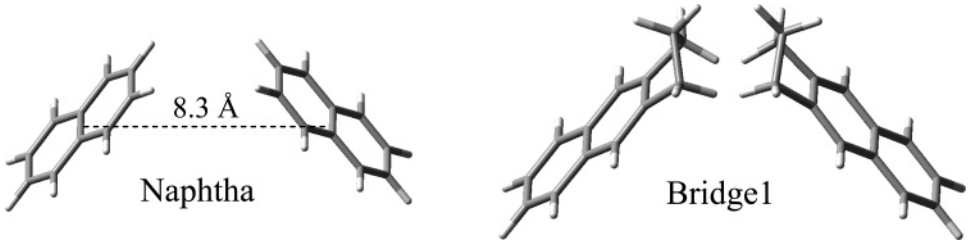

Figure 5. Two alternative molecular models used to represent the *D*/*A* pair in the perturbative calculation of DN4.

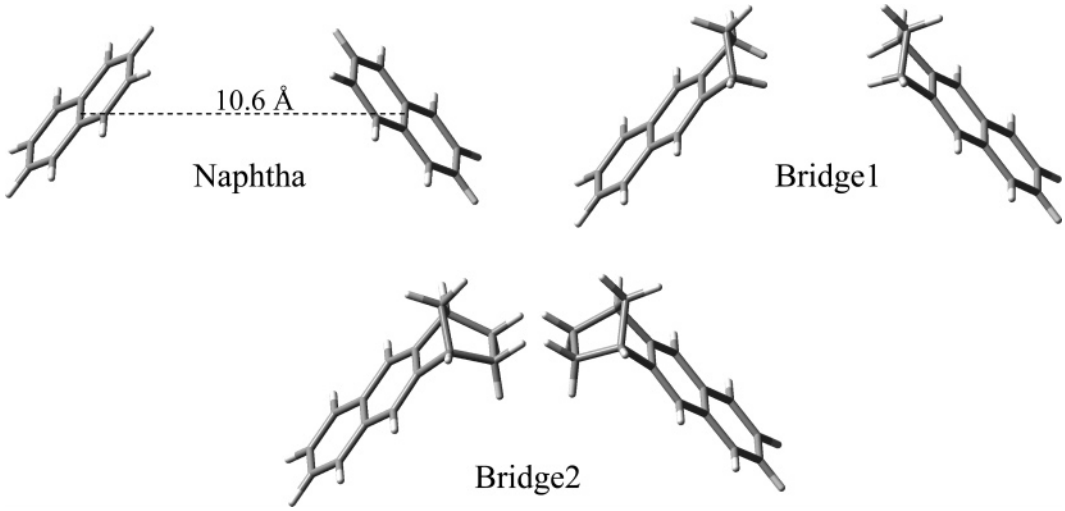

Figure 6. Three alternative molecular models used to represent the *D*/*A* pair in the perturbative calculation of DN6.

Table 3. ZINDO and TDDFT Dipole−Dipole Coupling $J^{(dd)}$ (in eV) Obtained Using the "Naphtha" Model System. Both Gas-Phase and Solvated Results are Reported

	DN2	DN4	DN6
		in gas	
ZINDO	0.314	0.133	0.060
TDDFT	0.219	0.093	0.043
		in hexane	
ZINDO	0.178	0.076	0.034
TDDFT	0.136	0.058	0.027

ZINDO approach but with significant underestimation of the experimentally observed values for all systems. This underestimation may be attributed to different reasons, among which the most important are the lack of real "through-bond" effects in the perturbative scheme and the accuracy of the ZINDO Hamiltonian used in these calculations. The "through-bond" effects will be better analyzed in the next section. Here, instead, we focus on the QM level by comparing ZINDO and TDDFT// DFT calculations.

For all the systems the use of TDDFT leads to an increase of the coupling toward a better agreement with the experiments. This behavior is explained by looking at the various terms forming the coupling (see eqs 6−8). We find that for all the compounds the leading term is the Coulomb one followed by the IEFPCM term (in solvated systems); both exchange-correlation and overlap terms are in fact almost negligible. By comparing these two dominant terms with the corresponding ones in ZINDO we find that the TDDFT Coulomb terms are always larger while the solvent terms are very similar in the two QM methods.

The differences between the simplified ZINDO description and the more complete TDDFT description can be further investigated by introducing a common modelization of the EET phenomenon in terms of the Förster[2] dipole−dipole approximation. In this framework the coupling becomes

$$J^{dd} = \frac{1}{n^2}\left[\frac{(\vec{\mu}_D^T \cdot \vec{\mu}_A^T)}{R^3} - 3\frac{(\vec{\mu}_D^T \cdot \vec{R})(\vec{\mu}_A^T \cdot \vec{R})}{R^5}\right] \qquad (9)$$

where $\vec{\mu}_D^T$ and $\vec{\mu}_A^T$ are the transition dipole moments of the *D* and *A* moieties, respectively, *R* is their distance, and the prefactor, $1/n^2$, where *n* is the refraction index of the solvent, accounts for the solvent screening effects (for isolated systems it reduces to the unity).

In Table 3 we report the dipole−dipole coupling J^{dd} in gas and in solution as obtained by using a ZINDO or a TDDFT description. For this analysis only the simplest model (the "Naphtha" model of Figure 4) is used for all the systems, it in fact becomes very difficult to extend such a description to the more complete Bridge1 and Bridge2 model systems in which the symmetry of the chromophore is broken and the electronic character of the transition is strongly perturbed.

Looking first at the gas-phase results we find that the differences between J^{dd} and $J^{(1)}$ (see the results for "Naphtha" model in Table 2) are larger for ZINDO than for TDDFT for which we find a very good correlation for all three systems. This might appear strange as in ZINDO the $J^{(1)}$ has only the Coulomb component, while in TDDFT exchange-correlation and overlap terms are also present. However, also for DN2 (e.g., where the two naphthalenes are closer), we observe that, while ZINDO J^{dd} is about 70% larger than the corresponding $J^{(1)}$, for TDDFT the differences reduce to less than 5%. This shows that ZINDO transition dipole moments are too large and thus careful attention has to be paid when semiempirical descriptions are used in combination with the dipole−dipole approximation. The good agreement found between TDDFT J^{dd} and $J^{(1)}$ in this system is due to the small values of the non-Coulomb terms; their effects can be seen noting that only for this system J^{dd} is slightly larger than $J^{(1)}$ as in the latter they oppose the Coulomb term.

It is interesting to note that, for J^{dd}, as well as for $J^{(1)}$, ZINDO and TDDFT become closer and closer when the two naphthalene systems are farther. In parallel, still passing from DN2 to DN4 and DN6 we observe that the differences between J^{dd} and $J^{(1)}$ become smaller both for ZINDO and for TDDFT. These results indicate that when the *D* and *A* are sufficiently far apart (i.e., they are not too strongly interacting), the level of calculation becomes less important and a simple dipolar description is sufficient to account for the largest part of the coupling.

When we introduce solvent effects, the picture becomes more complex; in fact, by using eq 9 to define the coupling, we adopt a further approximation besides that of representing the charge distributions as dipoles, e.g., that of representing the solvent effect as a simple screening factor $1/n^2$. The consequences of this further approximation can be evaluated by comparing Table 3 with those referring to the "Naphtha" model in Table 2. An interesting effect of the inclusion of the solvent is the reduction of the differences between J^{dd} and $J^{(1)}$ when computed at the ZINDO level and the parallel reduction between ZINDO and TDDFT J^{dd} values. Both these results are due to the same reason, i.e., the overestimation of the screening effect in the Förster dipole−dipole expression which counterbalances the overestimation of the ZINDO transition dipoles.

5. Through-Space vs Through-Bond

In this section we want to gain a better insight into the effect of the bridge on the EET coupling. To this end, we introduce two separated contributions. As already pointed out in section 4, the presence of the bridge modifies the electronic characteristics of the chromophores, reinforcing their transition dipoles and therefore contributing to the TS term in what we will denote as the "TS-bridge term". This term represents the increase in the coupling induced by the addition of pieces of the bridge to the interacting monomers and can be obtained for the DN4 and DN6 systems as the increase in $J^{(1)}$ (eq 6) when passing from the simplest "Naphtha" model to the "Bridge1" (DN4) or "Bridge2" (DN6) models. The second contribution induced by the bridge is what we will denote as the "real TB contribution"; this can be estimated as the difference between the experimental couplings and the $J^{(1)}$ values obtained for the "Naphtha", the "Bridge1", and the "Bridge2" models for DN2, DN4, and DN6 respectively, i.e., the models that, for each compound, include the largest piece of the bridge in the calculation of the perturbative couplings. Finally, we will indicate as "TS-naphtha" the TS term computed for the simplest "Naphtha" model.

The relative weights of these three terms (TS-bridge, TS-naphtha, and TB) of the total coupling are shown in Table 4 for solvated systems at both ZINDO and TDDFT levels.

Table 4. Relative Weights (in Percent) of the TB, TS-Naphtha, and TS-Bridge Terms of the Total Coupling for the Solvated Systems at TDDFT Level (Obtained by Comparison of Experimental and Perturbative Couplings)

	TS-naphtha	TS-bridge	TS	TB
		ZINDO		
DN2	41	0	41	59
DN4	25	9	34	66
DN6	24	17	41	59
		TDDFT		
DN2	53	0	53	47
DN4	34	15	49	51
DN6	30	34	64	36

The results reported in Table 4 show differences in the relative weights of the TS and TB contributions with respect to former studies,[11] where the TB term was considered as the dominant contribution for DN4 and DN6 systems. As a matter of fact we have to note that, generally, this TB term was computed as the difference between the coupling of the isolated naphthalene and what was observed for the bridged systems;[11] in such an analysis the details of the two different effects of the bridge (here indicated as TS-bridge and TB) were lost.

Here, instead we can distinguish between the effect of the bridge either to the reinforcement of the TS term and to the mediation of a real TB charge-transfer induced term. In this scheme, we find that, at the ZINDO level, the real TB contribution accounts for 66% and 59% of the total coupling in DN4 and DN6, respectively. A different result is found at the TDDFT level at which the TB term decreases to 51% and 36% for DN4 and DN6. These results show that the TB term is not the dominant contribution to the coupling in DN4 and DN6, as the large increase in the coupling induced by the presence of the bridge has to be interpreted in a more articulate way than usually done; the bridge in fact not only induces a TB term but also reinforces the TS interactions between the chromophores.

Both ZINDO and TDDFT results reported in Table 4 confirm the necessity to introduce an explicit term accounting for the TB contribution in order to provide a model with quantitative accuracy. In the study of intra-EET processes, the McConnell formula[42] has been derived to describe the indirect coupling between two identical chromophores mediated by a bridge. To this end, the bridge is divided in m units, and the TB mediated electronic coupling is given by

$$T_{\mathrm{TB}} \approx \left(-\frac{T^2}{A}\right)\left(-\frac{t}{A}\right)^{m-1} \tag{10}$$

where T is the chromophore-bridge coupling, t, the bridge-bridge coupling, and A, the energy gap between chromophore and bridge configurations. A detailed analysis of the approximations inherent in the McConnell model and its range of applicability has been given by Jordan and Paddon-Row (see ref 8c), who reviewed different strategies to study the interactions responsible for long-range mediated electronic coupling between chromophores attached to rigid polynorbornyl bridges. For long bridges, the McConnell model predicts an exponential attenuation of the magnitude of electronic coupling with increasing bridge length, measured as the number of sigma bonds separating the donor and the acceptor chromophores, namely:[14]

$$T_{\mathrm{TB}} = T_0 \exp[-\beta(m - m_0)] \tag{11}$$

where T_0 is the TB electronic coupling for m_0 bridge units (or bonds) and β is the decay constant (per bond) which describes the attenuation of the coupling with distance.

If we apply eq 11 to the TB contributions obtained from the previous analysis (see Table 4), we can obtain the T_0 coefficient and the β exponent by linear regression of the equation $\ln T_{\mathrm{TB}} = \ln T_0 - \beta(m - m_0)$, considering as T_0 the TB contribution computed for DN2. Indeed, the TB contribution obtained from the ZINDO calculations in hexane is found to follow an exponential decay with the number of bonds (with correlation coefficient r equal to 0.9777) characterized by a β value of 0.34. A good exponential behavior is also found for the TDDFT TB contributions ($r = 0.9712$) for which a β value of 0.40 is found. These values of the decay constant β are significantly smaller than what was previously reported (namely 1.01 and 0.91) for similar compounds:[14] we note however that these latter referred to the splitting of different excited states (namely the first and second excited singlet electronic states of the naphthyl, here Bridge2, monomer) and they were obtained in gas phase. For example, if we repeat the evaluation of β using gas-phase data, also in the present case we find larger values, namely 0.44 at the ZINDO level and 0.51 at the TDDFT level.

6. The Supermolecule Approach

In section 4 we have shown that the perturbative scheme, even when in its most accurate TDDFT version, gives coupling values always smaller than the experiments. More in detail, such an underestimation becomes greater when shorter bridges are present: while for DN6 we obtain a quite good agreement between calculated and measured couplings, for DN2 the calculated value is about one-half the experimental one.

This behavior, as well as the analysis reported in the previous section, clearly shows that for shorter bridges the perturbative approach is not sufficient as large electronic delocalization between chromophores takes place. To quantitatively evaluate this delocalization, we can calculate the couplings for the complete DNX systems (i.e., apply the supermolecule approach) by solving their TDDFT (or ZINDO) eq 2 in an exact way.

Before doing this analysis, however, it is interesting to check the reliability and the accuracy of the perturbative results by applying the supermolecule approach to the same model systems used in the perturbative approach (see Figure 4−6) but this time solving in an exact way their TDDFT (or ZINDO) equations. The resulting splittings when compared with the corresponding $J^{(1)}$ show an almost exact equivalence for all systems at either the ZINDO or TDDFT level. This is clear proof of the validity of the perturbative approach but also of the absence of any "direct through-space orbital overlap" (involving charge transfer) between the two monomers. In fact, if such interactions were present then they would have induced differences between the perturbative and the supermolecule couplings, as in the latter we have "exactly" accounted for all possible $D-A$ interactions while in the former we have simply combined the densities of D and A as computed in the absence of their interaction.

We can now proceed to the real DNX systems and calculate their couplings. The results obtained at the ZINDO and TDDFT levels are reported in Table 5 for the isolated and solvated systems.

(42) McConnell, H. M. *J. Chem. Phys.* **1961**, *35*, 508.

Table 5. Superpermolecule ZINDO and TDDFT Couplings (in eV) for DNX Systems in Gas Phase and in Solution

	ZINDO	TDDFT
	in gas	
DN2	0.333	0.543
DN4	0.144	0.440
DN6	0.077	0.156
	in hexane	
DN2	0.303	0.513
DN4	0.110	0.372
DN6	0.050	0.115

Table 6. Calculated and Experimental Excitation Energies (in eV) for DNX Systems in Hexane

	ZINDO	TDDFT	exp[a]
DN2	4.45/5.06	4.70/5.73	5.00/5.76
DN4	4.74/4.96	4.87/5.61	5.21/5.65
DN6	4.81/4.91	5.19/5.41	5.34/5.54

[a] Reference 11.

The comparison with the experiments for the solvated systems shows an underestimation of the ZINDO couplings for all the systems but with a much better agreement for DN2 (underestimated only by 20%) than for DN4 and DN6 (whose couplings are underestimated by about 50%). By contrast, the TDDFT couplings are always larger than the observed ones; in particular the TDDFT value is 35%, 66%, and 16% larger than the experimental values for DN2, DN4, and DN6, respectively.

To better understand such an opposite behavior it is useful to compare the transition energies of the two split states with the experimental absorption spectra. Such a comparison is reported in Table 6.

From Table 6, it appears evident that the overestimation of the coupling at the TDDFT level is due to an unbalanced description of the two states, being the lowest too stabilized, especially for DN2 and DN4. We also note that at the TDDFT level the analysis of the coupling is complicated due to the presence of energetically low-lying excited states with large oscillatory strengths which are not observed in the experimental spectra. In particular, what we have found in all three systems is a highly permitted "intruder" state with a transition dipole moment parallel to the direction of the bridge main axis exactly as the lowest split state and in fact both states present a significant contribution from an occupied orbital mainly localized on the bridge; conversely, an analogous transition cannot be found in the enlarged Bridge1 or Bridge2 models.

These findings might seem unexpected, given the excellent agreement obtained for the TDDFT transition energies of both naphthalene (see section 3) and the chromophore used in the "Bridge2" model system (for which the calculated excitation energy in hexane is 5.45 eV, exactly as experimentally observed). As a matter of fact, these difficulties of TDDFT are not completely new. Reimers and co-workers,[43] in a study on the electronic absorption spectra of oligoporphyrins, found various nonobserved transitions of high intensity between the valence *Q* and *B* bands typical of porphyrinic systems. In such a study, it was also shown that these spurious states were still present when asymptotically corrected functionals[44] were used. It has certainly to be noted that the systems studied by Reimers and co-workers were highly π-conjugated (being the porphyrins linked by conjugated tetra-aza-anthracene bridge), while in our case the bridge breaks the conjugation; however the resemblances found seem to indicate that a similar problem exists in the two studies.

It is also interesting to recall that TDDFT problems in the description of the energetic position of the excited states of complexes showing excitation-energy transfers were also shown in studies on various molecular complexes of biological relevance. In those cases, however, the artificially low-lying states found presented clear charge-transfer character.[23,25] The error in the excitation energies of these CT excited states was traced back to the self-interaction error present in the orbital energies of the DFT calculation, which leads to an underestimation of the HOMO−LUMO gap.[23] Our systems (and the studied transitions) are obviously different from these CT systems, but still some suggestions proposed to correct the wrong behavior can be also checked here. In particular, Head-Gordon and coworkers[45] suggested a hybrid scheme combining TDDFT with CIS (or TDHF). In fact, in contrast to TDDFT methods, CIS and TDHF yield the correct behavior of the CT states because of the full inclusion of HF exchange, which leads to the cancellation of electron-transfer self-interaction. On the other hand, the excitation energies calculated with CIS or TDHF are usually much too large because of the lack of dynamic correlation. Therefore, the combination of the two methods should allow us to obtain reasonable estimates for the energies of CT states relative to valence-excited states. This was originally formulated to obtain the asymptotically correct potential energy curve for CT states, but we can try to reformulate it for our specific problem of the EET coupling in the following way. The corrected transition energies, $\omega_{\pm}^{\mathrm{corr}}(DNX)$, for the split states of DNX systems are obtained by shifting the CIS results, $\omega_{\pm}^{\mathrm{CIS}}(DNX)$, by the difference obtained in the reference transition energy of the proper *Donor* (and *Acceptor*) chromophore at the TDDFT (ω^{TDDFT}) and CIS (ω^{CIS}) level, namely:

$$\omega_{\pm}^{\mathrm{corr}} = \omega_{\pm}^{\mathrm{CIS}} + (\omega^{\mathrm{TDDFT}} - \omega^{\mathrm{CIS}}) \qquad (12)$$

In this way we can in fact combine the accuracy of TDDFT in describing the excitation energies of the model chromophore (either naphthalene or naphthalene complemented by pieces of the bridge) with the more balanced CIS description of the states in the complete systems. This simple scheme, when applied to the three DNX systems in hexane, leads to $\omega_{\pm}^{\mathrm{corr}} = 5.17/6.04$ eV for DN2, $\omega_{\pm}^{\mathrm{corr}} = 5.27/5.66$ eV for DN4, and $\omega_{\pm}^{\mathrm{corr}} = 5.36/5.52$ eV for DN6 which well agree with the experimental data reported in Table 6.

It is obvious that when we pass from the absolute transition energies to their differences (e.g., the coupling), the correction ($\omega^{\mathrm{TDDFT}} - \omega^{\mathrm{CIS}}$) disappears as it is constant for both states and thus the corrected coupling coincides with the CIS coupling, namely 0.44, 0.20, and 0.08 eV for DN2, DN4, and DN6, respectively. By recalling the experimental data of 0.38, 0.22, and 0.1 eV, it appears evident that the calculated splittings are now accurate along the whole series of compounds. It is also

(43) Cai, Z.-L.; Sendt, K.; Reimers, J. R. *J. Chem. Phys.* **2002**, *117*, 5543.
(44) Hamprecht, F. A.; Cohen, A. J.; Tozer, D. J.; Handy, N. C. *J. Chem. Phys.* **1998**, *109*, 6264.
(45) Dreuw, A.; Weisman, J. L.; Head-Gordon, M. *J. Chem. Phys.* **2003**, *119*, 2943.

worth noting that the artificial intense low-lying states appearing at TDDFT level still exist but this time they are much weaker than the others.

7. Density Maps

As a final analysis we present a graphical representation of the couplings in terms of the transition density maps originally introduced by Tretiak and Mukamel.[16]

Density matrices establish a natural connection between electronic structure and the molecular optical response. The ground-state density matrix is widely used in various types of population analysis to prescribe a charge to specific atoms and are commonly visualized using contour charge density maps. The off-diagonal elements, known as bond orders, represent the bonding structure associated with a pair of atomic orbitals and are useful for interpreting the chemical bonding pattern across the molecule. In an analogy with such ground-state maps, contour maps built from the electronic transition density matrices permit us to visualize the probabilities of an electron moving from one molecular position or atom (horizontal axis) to another one (vertical axis) for a transition from the ground state to a particular excited state.

Here we present the transition density contour plots for the two extremes (DN2 and DN6) of the set of DNX systems obtained using either the perturbative model or the "exact" supermolecule; the same plots for the DN4 system are reported in the Supporting Information.

Both ZINDO and TDDFT results are shown, whereas we limit them to the solvated systems only. In the perturbative model the plots have been realized using a transition density matrix obtained by projecting the *Donor* and *Acceptor* transition density matrices of the band involved in the splitting in the space of the corresponding complete DNX system by using zeros in the off-diagonal blocks: for DN2 the "Naphtha" model has been used, while for DN6 the "Bridge2" model has been used (see Figures 4 and 6). For the supermolecule, the transition densities of the two split states are reported. The axis labels correspond to the atom numbering shown in the molecular structures reported in Figure 7. Note also that hydrogens are omitted as their contributions are typically negligible. Color variations away from the main diagonal represent photoinduced electron transfer. Red, green, and blue signify low, intermediate, and high probabilities, respectively.

The ZINDO maps (Figure 7) obtained from the perturbative model show a similar picture for the three systems, characterized by induced charges in atoms 1−2 and 9−10 at the ends of the naphthalene moieties. The introduction of the bridge (when passing from the "naphtha" model of DN2 to the bridged model used for DN6) does not substantially alter the picture, but the appearance of off-diagonal contributions introduces in the transition a weak electron transfer character from the bridge to the naphthalene. Interestingly, the comparison of these maps with those obtained for the "exact" supermolecule permits us to immediately assess the reliability of the perturbative model in the description of the excitations involved in the coupling. As already pointed out by Mukamel and co-workers,[15] the interaction giving rise to the coupling in DN6 is, at least at the ZINDO level, completely electrostatic and relatively weak. In fact, the map for the perturbative model is very similar to those obtained in the supermolecule; this confirms the validity of the

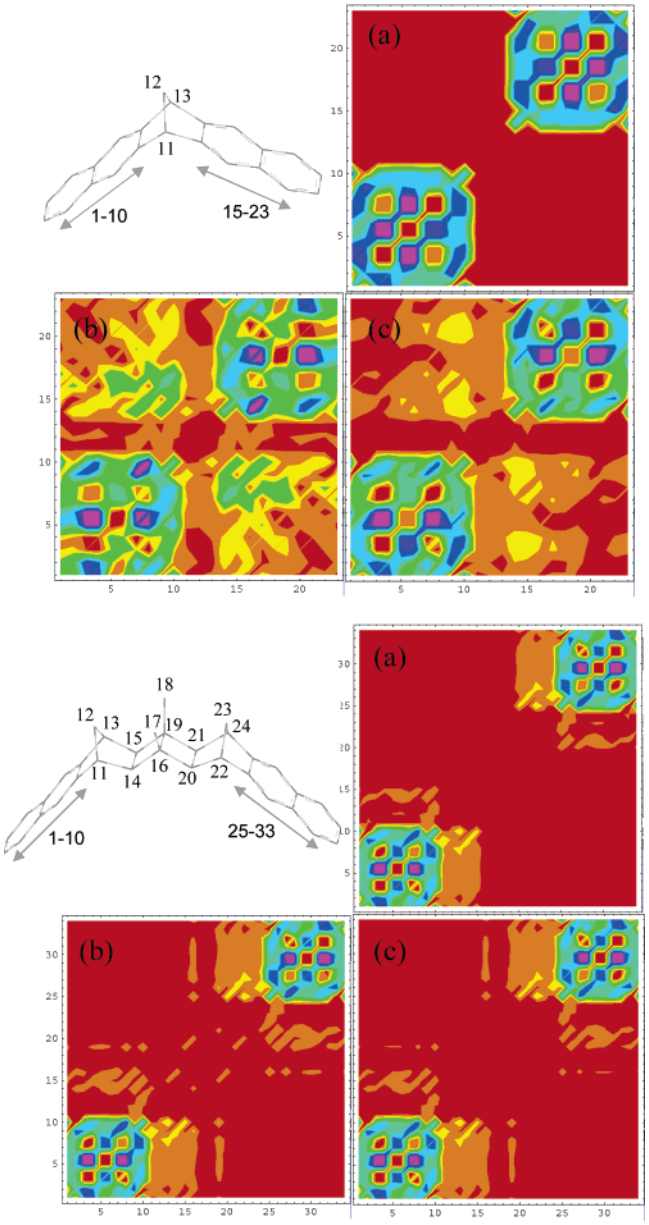

Figure 7. ZINDO transition density contour plots for DN2 (above) and DN6 (below) obtained using either the perturbative model (plot (a)) or the "exact" supermolecule. For the supermolecule, the transition densities of the two split states are reported (plots (b) and (c)). The axis labels correspond to the atom numbering shown in the molecular structure.

exciton model in this case. On the other hand, for DN4 (reported in the Supporting Information) a more delocalized character of the transition begins to show up, as indicated by the appearance of off-diagonal elements accounting for electron transfers between the two monomers in the two maps referring to the split excited states. As these charge-delocalization effects are possible only due to the presence of the bridge, the map of the perturbative approach does not present them. However, the general picture of the excitation is recovered by such an approximated method. Finally, the map obtained for DN2 is characterized by a strong electron delocalization which breaks the exciton picture on which the perturbative approach is based.

The clear and simple analysis of the ZINDO maps is largely complicated at TDDFT level as shown in Figure 8.

The main difference is that now the bridge participates much more effectively in the excitation, while at the ZINDO level

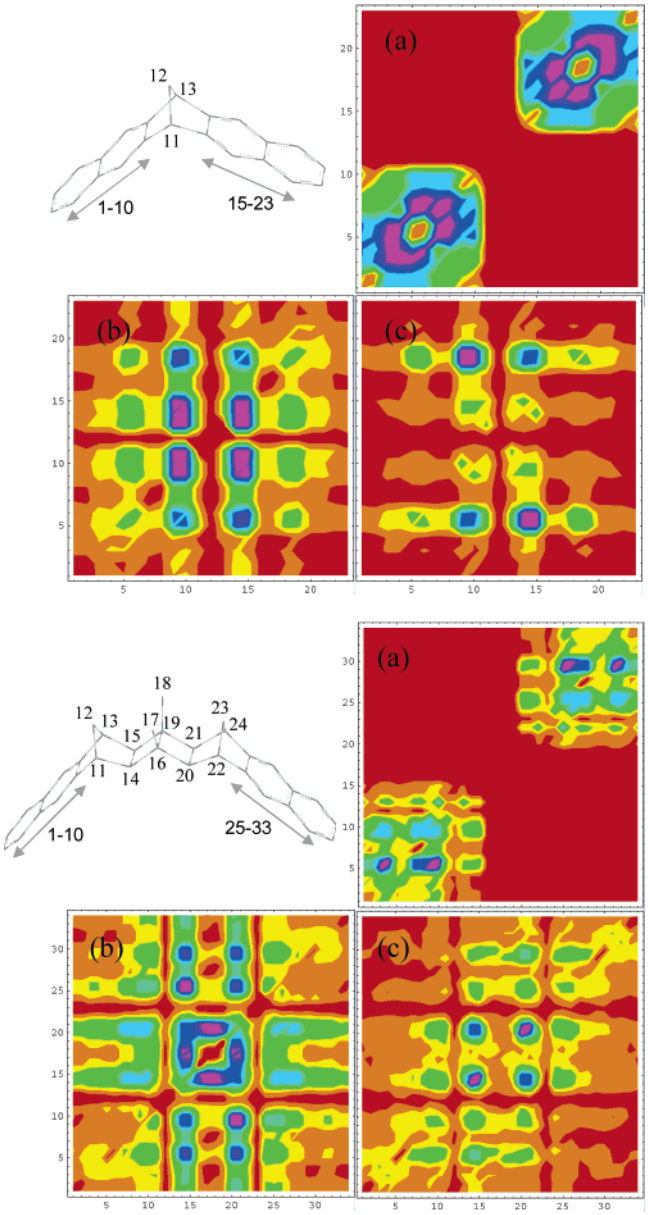

Figure 8. TDDFT transition density contour plots for DN2 (above) and DN6 (below) obtained using either the perturbative model (plot (a)) or the "exact" supermolecule. For the supermolecule, the transition densities of the two split states are reported (plots (b) and (c)). The axis labels correspond to the atom numbering shown in the molecular structure.

the transitions are always almost completely localized in the naphthalene moieties. This active participation of the bridge leads to a transition that is no longer of purely $\pi-\pi^*$ character. This evidence is supported by the analysis of the orbitals participating in the excitations, now including significant contributions from occupied orbitals in large part localized on the bridge.

Another important difference found for these maps, when compared to the simple ZINDO pictures, is that a strong electronic delocalization is found not only for DN2 but also for DN4 and DN6, an effect that obviously cannot be reproduced by the perturbative approach.

To understand these findings we have to recall what was reported in section 6 about the differences found between the TDDFT supermolecule computations and the experimental data. There, we have discussed possible reasons for these differences and noted that the presence of the bridge between the two naphthalenes leads to an incorrect description of the states polarized along the bridge main axis like the lowest one in the split pair (state (b) in the figures). As a result such a state presents an artificial overestimation of the contribution of the bridge atoms which is not observed in the model systems not even when a large part of the bridge is included like in the Bridge2 model. This unbalanced description of the electronic nature in the DNX systems is reflected in the large differences between the perturbative and the complete maps at the TDDFT level.

8. Summary

In this paper we have presented a computational strategy aimed at both identifying the physical aspects beyond the EET coupling and quantifying their relative weights. Such a strategy involves different steps, first a check on the quality of the QM level has to be done on the excitation energies of the involved chromophores, then a perturbative solution of the response scheme at such a level is used to obtain the TS contribution of the coupling. Third, by comparing the calculated couplings with the experimental ones, an empirical expression for the TB contribution is determined and extended to study the same process in other correlated systems.

The advantages of this strategy are of different natures. The first advantage is that we have not introduced any "a priori" definition on the nature of the interactions between the two chromophores but instead we compute their coupling within a scheme coherently accounting for different kinds of interactions (namely, direct and indirect, i.e., solvent-mediated-Coulomb exchange, possibly including also correlation effects, and overlap interactions). In addition, from a computational point of view, the most expensive calculations are on the two separated chromophores (in our case just a single calculation is necessary as $D \equiv A$) and not on the complete system, whereas the determination of their coupling only requires an easy and fast calculation of integrals which can be performed with standard numerical integration techniques. Finally, the use of separated chromophores prevent all the difficulties often involved in the accurate calculation of excitation energies of the complete systems.

Obviously, the main goal of this approach is not the exact reproduction of the experimental data but instead their interpretation. However, we have also shown that empirical (or modelistic) corrections can be easily introduced to account for the missing interactions (such as the through-bond effects) making the approach useful also as a predictive tool. Note that for nonbonded *D*/*A* pairs, i.e., for intermolecular EET processes, this predictive capability becomes powerful as the perturbative approach becomes "exact" (i.e., no important terms are neglected) still maintaining both the simplicity and the computational effectiveness.

In parallel to this interpretative analysis we have tested two of the most used QM approaches, the semiempirical ZINDO and the TDDFT, to show the difficulties that their standard application to the study of the EET processes hides.

On one hand, we have shown that the ZINDO approach despite its computational effectiveness has to be used with caution at least in these bichromophoric bridged systems; the splittings are in fact always too low showing thatthe ZINDO

description can only account for a part of the effect. In addition, we have shown that the overestimation of the ZINDO transition dipole moments can lead to an erroneous estimation of the dipole−dipole contribution to the coupling as well as of the solvent effects.

On the other hand, we have shown that the use of standard TDDFT functionals can correctly (and very accurately) predict the transition properties and energies of the single chromophores but they present serious difficulties in determining the correct position (and the correct electronic nature) of the excited states in the complete systems. In this case, the splitting is always too large due to an unbalanced description of the two involved excited states. Finally, a simple but effective hybrid approach combining TDDFT and CIS results has been used to achieve a more accurate description of both the EET couplings and the position of the split excited states.

Acknowledgment. The authors thank Professor Jacopo Tomasi and Professor Roberto Cammi for their continuous help and for the useful discussions on both theoretical and numerical aspects.

Supporting Information Available: Geometries (Cartesian coordinates) and energies of DN2, DN4, and DN6 at the ZINDO and DFT level; ZINDO and TDDFT transition density plots for the DN4 system; complete ref 38. This material is available free of charge via the Internet at http://pubs.acs.org.

JA055489G